Title

Separation of extra- and intracellular metabolites using hyperpolarized 13C diffusion weighted MR

Authors

Koelsch, Bertram L

Sriram, Renuka

Keshari, Kayvan R

et al.

Publication Date

2016-09-01

DOI

10.1016/j.jmr.2016.07.002

Peer reviewed

Journal of Magnetic Resonance 270 (2016) 115–123

Contents lists available at ScienceDirect

Journal of Magnetic Resonance

journal homepage: www.elsevier.com/locate/jmr

Separation of extra- and intracellular metabolites using hyperpolarized ^{13}C diffusion weighted MR ☆

Bertram L. Koelsch [a,b], Renuka Sriram [a,*], Kayvan R. Keshari [c,d], Christine Leon Swisher [a,b], Mark Van Criekinge [a], Subramaniam Sukumar [a], Daniel B. Vigneron [a,b], Zhen J. Wang [a], Peder E.Z. Larson [a,b], John Kurhanewicz [a,b]

[a] Radiology and Biomedical Imaging, University of California San Francisco, San Francisco, CA, USA
[b] UC Berkeley–UCSF Graduate Program in Bioengineering, University of California, Berkeley and University of California, San Francisco, CA, USA
[c] Radiology and Molecular Pharmacology Program, Memorial Sloan Kettering Cancer Center, New York, NY, USA
[d] Weill Cornell Medical College, New York, NY, USA

ARTICLE INFO

Article history:
Received 24 May 2016
Revised 6 July 2016
Accepted 7 July 2016
Available online 9 July 2016

Keywords:
Hyperpolarized ^{13}C magnetic resonance (HP ^{13}C MR)
Dynamic nuclear polarization (DNP)
Diffusion weighted magnetic resonance
Pyruvate
Lactate
Aerobic glycolysis
Cellular transport
Lactate efflux
Renal cell carcinoma (RCC)
Cancer aggressiveness
Cancer

ABSTRACT

This work demonstrates the separation of extra- and intracellular components of glycolytic metabolites with diffusion weighted hyperpolarized ^{13}C magnetic resonance spectroscopy. Using *b*-values of up to 15,000 s mm^{-2}, a multi-exponential signal response was measured for hyperpolarized [1-^{13}C] pyruvate and lactate. By fitting the fast and slow asymptotes of these curves, their extra- and intracellular weighted diffusion coefficients were determined in cells perfused in a MR compatible bioreactor. In addition to measuring intracellular weighted diffusion, extra- and intracellular weighted hyperpolarized ^{13}C metabolites pools are assessed in real-time, including their modulation with inhibition of monocarboxylate transporters. These studies demonstrate the ability to simultaneously assess membrane transport in addition to enzymatic activity with the use of diffusion weighted hyperpolarized ^{13}C MR. This technique could be an indispensible tool to evaluate the impact of microenvironment on the presence, aggressiveness and metastatic potential of a variety of cancers.

1. Introduction

The use of hyperpolarized ^{13}C pyruvate has shown clinical potential in identifying and characterizing tumors by measuring its real-time conversion to hyperpolarized ^{13}C lactate [1]. These measurements are a direct consequence of increased glycolysis, a hallmark of cancer cells [2]. Studies in pre-clinical animal models of cancers have shown increased hyperpolarized ^{13}C lactate production with increasing cancer grade and aggressiveness [3]. Another common feature of aggressive and metastatic cancer cells is an acidic extracellular environment [4], a process that promotes tumor growth and invasion. This acidification is, in part, due to increased tumor lactate production and higher lactate efflux via the upregulated monocarboxylate transporter 4 (MCT4) [5,6], which co-transport lactate and protons out of the cell. Thus, measuring not only the overall production of hyperpolarized ^{13}C lactate, but also its transport may improve the ability to non-invasively identify aggressive tumors with high metastatic potential using hyperpolarized ^{13}C MR.

A prior publication has shown that hyperpolarized ^{13}C pyruvate can be used to differentiate human metastatic renal cell carcinoma (RCC) cells from indolent RCC cells using an *ex vivo* MR-compatible

Abbreviations: ADC, apparent diffusion coefficient; MR, magnetic resonance; MRS, magnetic resonance spectroscopy; DNP, dynamic nuclear polarization; RCC, renal cell carcinoma; DMEM, Dulbecco's Modified Eagle's medium; DIDS, 4,4′-Diiso thiocyanostilbene-2,2′-disulfonic acid; MCT, monocarboxylate transporter; LDH, lactate dehydrogenase; TCA, tricarboxylic acid; L_{intra}, intracellular lactate; L_{extra}, extracellular lactate; L_{total}, total lactate; P_{intra}, intracellular pyruvate; P_{extra}, extracellular pyruvate; P_{total}, total pyruvate; DMSO, dimethyl sulfoxide.

☆ Grant Sponsor: National Institutes of Health (R01 EB013427, R01 EB017449, R01 CA183071, R01 EB016741, P41 EB013598, R21 EB005363, R00 EB014328, P30 CA008748 and R01 CA166655) and Department of Defense (USAMRMC CA110032).

* Corresponding author at: University of California, San Francisco, Byers Hall, Room 201B, 1700 4th Street, MC 2520, San Francisco, CA 94158, USA.
E-mail address: renuka.sriram@ucsf.edu (R. Sriram).

http://dx.doi.org/10.1016/j.jmr.2016.07.002
1090-7807/

bioreactor, a cell perfusion system [7]. In that *ex vivo* study, metastatic RCC UOK262 cells rapidly transported hyperpolarized ^{13}C lactate out of the cells during the course of the hyperpolarized ^{13}C MR experiment [7]. Additionally, it was recently shown that the extra- and intracellular hyperpolarized ^{13}C lactate signal can be directly measured in RCC cells in the same bioreactor system, and confirmed that the metastatic RCC cells have higher extracellular lactate pool [8]. By correlating the hyperpolarized lactate signals to the relative expression levels of MCT4 between the indolent and metastatic RCC cells, these studies demonstrated that the localization of hyperpolarized ^{13}C lactate between the extra- and intracellular environment could provide valuable information concerning tumor aggressiveness and metastatic potential. However, these previous *ex vivo* studies relied on the detection of small frequency shifts, which cannot be directly translated to *in vivo* imaging due to challenges in obtaining sufficient spectral resolution.

Diffusion weighted MR has been extensively used to assess the localization of various metabolites, both *in vitro* to study their extra- and intracellular distributions and *in vivo* to characterize tumor tissue microstructure based on water's apparent diffusion coefficient (ADC) [9]. Recently, there have been several publications that have used diffusion weighted MR to measure the diffusion coefficients of hyperpolarized ^{13}C metabolites, in solution [10], in cell suspensions [11] and *in vivo* [12–14]. These studies showed how changes in the ADCs could indicate the extra- and intracellular localization of the hyperpolarized ^{13}C metabolites. Yet, each of these studies used relatively small diffusion weighting gradients, or *b*-values, and thus measured only single diffusion coefficients from mono-exponential signal responses that did not provide extra- and intracellular separation. Proton diffusion studies have shown that using a wide range of *b*-values, with large values upwards of 3000 s mm^{-2}, results in a multi-exponential signal response that is indicative of the various diffusion environments, both *in vitro* in cells [15,16] and *in vivo* [17].

In the studies presented here, large diffusion gradients were used to investigate the extra- and intracellular weighted distribution of hyperpolarized [1-^{13}C] pyruvate and its metabolites in RCC cells perfused in a MR compatible 3D cell culture bioreactor. Using *b*-values up to 15,000 s mm^{-2}, a multi-exponential signal response was measured for the various hyperpolarized ^{13}C metabolites and by fitting the fast and slow asymptotes of these curves, their extra- and intracellular weighted diffusion coefficients were determined. Additionally, the dynamics of these extra- and intracellular weighted hyperpolarized ^{13}C metabolite pools were assessed in real-time, including a demonstration of the effect of inhibiting MCT4 mediated efflux of hyperpolarized ^{13}C lactate. These studies demonstrate the importance of membrane transport, in addition to enzymatic activity, in understanding the metabolic flux of hyperpolarized ^{13}C metabolites. As opposed to previous diffusion weighted studies of hyperpolarized ^{13}C metabolites, both the high *b*-values used in this study and the large difference between the intra- and extracellular diffusion environments, which allow for a more thorough separation of the two signal pools, provide a measurement of the intracellular weighted diffusion coefficients that may be closer to the true intracellular diffusion coefficient. This improved intracellular weighted lactate ADC measured in this work may aid the design and interpretation of future *in vivo* diffusion weighted imaging clinical studies.

2. Methods

2.1. RCC cell line experiments in an NMR compatible bioreactor

Two different renal cell carcinoma (RCC) cell lines were used. UMRC6 cells are representative of localized human clear cell RCC [18], and were a gift from Dr. Bart Grossman (MD Anderson Cancer Center, Houston, TX; obtained January, 2010; authenticated using STR profiling, October 2012). UOK262 cells are derived from a metastasis of the highly aggressive hereditary leiomyomatosis RCC (HLRCC), which is characterized by mutation of the TCA cycle enzyme fumarate hydratase [19]. UOK262 cells were a gift from Dr. W. Marston Linehan (National Cancer Institute, Bethesda, MD; obtained May, 2010; authenticated using STR profiling, October 2012). All cells were grown in Dulbeco's Modified Eagle's Medium (DMEM) with 4.5 g L^{-1} glucose. The cells were passaged serially and were used for assays and magnetic resonance experiments between passages 2 to 10 and at 60–80% confluency.

For bioreactor experiments, cells were electrostatically encapsulated into 3.5% w/v alginate microspheres, as previously described [20,21], and then loaded into an NMR spectrometer compatible bioreactor [7,20]. Cell-free alginate microspheres were created by the same process. Approximately 800 μL of either cell-free microspheres or microspheres with cells were loaded into the bioreactor. Only for the ^{1}H diffusion weighted imaging experiment (see below) the microspheres with and without cells were layered into the bioreactor (Fig. 2b). The bioreactor was perfused with DMEM H-21 media at a flow rate of 2 mL min^{-1} and kept at 37 °C with water-jacketed perfusion lines and 95% air/5% CO_2 with a gas exchanger.

All MR studies were performed on a 14.1 T Varian INOVA spectrometer (600 MHz ^{1}H/150 MHz ^{13}C) microimaging system (Agilent Technologies), equipped with a 10 mm broadband probe and 100 G cm^{-1} gradients. Probe temperature was controlled at 37 °C. ^{31}P spectra were acquired before and after each hyperpolarized study to assess cell viability and measure the number of cells within the bioreactor, as previously described [7]; TR = 3 s, 512 or 1024 averages, 90° flip-angle.

2.2. Diffusion weighted studies of ^{1}H water

A ^{1}H pulsed gradient single spin echo sequence with rectangular 90° and 180° RF pulses was used to measure the extra- and intracellular diffusion coefficients of water: TR = 2.5 s, TE = 26 ms, gradient pulse duration δ = 9 ms, gradient pulse separation Δ = 16 ms and without averaging. The diffusion weighting or *b*-value was arrayed by changing the gradient amplitudes *G* from 0 to 46 G cm^{-1}, resulting in *b*-values 0–15,944 s mm^{-2}. Diffusion gradients were applied in the transverse direction, i.e., G_x or G_y. The flow was stopped for the duration of these scans to eliminate the effects of flow.

The diffusion coefficients of extra- and intracellular weighted water was determined by fitting the first 7 points (i.e., fast decaying asymptote) or last 7 points (i.e., slowly decaying asymptote) of the multi-exponential signal response to the equation [16,22]

$$\ln(S_i/S_0) = -b \cdot D \tag{1}$$

where S_i is the signal at a specific *b*, or diffusion weighting, S_0 is the signal without diffusion weighting and *D* is the diffusion coefficient. The *b*-value is defined as:

$$b = n\gamma^2 G^2 \delta^2 (\Delta - \delta/3) \tag{2}$$

in which γ is the gyromagnetic ratio and *n* is 1 for single spin echo experiments and 2 for double spin echo experiments, used here for ^{1}H and ^{13}C experiments, respectively. Since the system's maximum slew rate was used, the effect of the gradient ramps were negligible on total *b*-value and hence were neglected from these calculations. For the cell-free alginate microspheres, only the fast decaying asymptote was calculated.

For these experiments, a three-way analysis of variants (ANOVA) was used to identify statistical differences between extracellular weighted diffusion coefficients, followed by a Tukey's

HSD test where appropriate to make pair-wise comparisons. A paired two-tailed t-test was used to compare intracellular weighted diffusion coefficients between the two cell lines. For all comparisons the significance level (α) was 0.05. All values are represented as mean ± standard deviation. Experiments were performed in quadruplicates. Normality was tested with the Shapiro–Wilk test. All statistical comparisons were done in R, version 3.2.4.

A ^{1}H diffusion weighted spin echo imaging sequence was used to visually show the suppression of the extracellular water signal with increasing *b*-values. Again, only the gradient amplitude was changed to increase the diffusion weighting, while the gradient timing parameters were kept constant: δ = 6 ms, Δ = 14 ms. TR = 2 s, TE = 27.7 ms, FOV = 40 mm × 8 mm (RO × PE), 256 × 64 matrix, 0.5 mm slices and 10 or 100 averages. These experiments were performed in quadruplicates.

2.3. Hyperpolarization of ^{13}C metabolites

A HyperSense (Oxford Instruments) was used for dynamic nuclear polarization (DNP), operating at 3.35 T, 1.3 K and 94.100 GHz microwave irradiation for a minimum of 45 min. Sample preparation and polarization methods are similar to those previously published [23–25]. The [1-^{13}C] pyruvate preparation contained 14.1 M neat pyruvic acid, 16.5 mM of the trityl radical OX063 (GE Healthcare) and 1.5 mM Dotarem (Guerbet). After polarization, ^{13}C pyruvate was dissolved with 5 mL of a 50 mM phosphate-buffer, yielding a final concentration of 21.15 mM. Studies with cell-free alginate microspheres were done with ^{13}C pyruvate and ^{13}C lactate. The [1-^{13}C] lactate preparation contained equal parts glycerol and a 50% by weight solution of sodium [1-^{13}C] lactate, 15 mM of the trityl radical and 1 mM Dotarem; lactate was at a final concentration of 15 mM in the dissolution solution. After dissolution, 1 mL of the hyperpolarized solution was immediately injected into the bioreactor over 30 s.

2.4. Diffusion weighted pulse sequence for hyperpolarized ^{13}C

A pulsed gradient double spin echo sequence was used for all hyperpolarized ^{13}C diffusion experiments, as seen in Fig. 1a [10]. The pulsed gradient double spin echo sequence was chosen for the diffusion weighting of hyperpolarized ^{13}C metabolites, given that it has several advantages. The adiabatic pulses used are insensitive to a range of RF field (B_1) strengths. Spectral phase is eliminated with a pair of adiabatic refocusing pulses, where the second refocusing pulse re-winds any non-linear phase imparted by the first [26]. The pair of refocusing pulses also places the hyperpolarized magnetization back onto the +*z* axis before the next excitation, which over the time course of the experiment prevents mixing of hyperpolarized magnetization that is oriented along the +*z* and −*z* axes that would lead to rapid signal loss [27].

The use of two pairs of diffusion gradients for this diffusion sequence also has several advantages. First, the relatively small gyromagnetic ratio of ^{13}C nuclei reduces diffusion weighting, as seen by Eq. (2). Hence, the use of two pairs of diffusion gradients doubles the *b*-value, allowing for the generation of *b*-values up to 15,000 s mm^{-2}. Additionally, the two pairs of diffusion gradients will minimize the diffusion time ($\Delta - \delta/3$) necessary to achieve a desired *b*-value, since each gradient pair will separately de- and re-phase the magnetization. This minimizes the effects of a restricted environment (i.e., cells) in the diffusion coefficient measurements [15], where longer diffusion times would lead to decreases in the measured diffusion coefficient [28]. In the studies discussed here, the diffusion times are kept constant, 13 ms for ^{1}H studies and 26.7 ms for ^{13}C studies, while the gradient amplitudes are changed to increase the diffusion weighting. While these are relatively short diffusion times, the diffusion coefficients presented here are still apparent diffusion coefficients since there will inevitably still be some restricted diffusion effects.

A 15° or 30° excitation pulse was used in combination with a pair of 180° hyperbolic secant adiabatic refocusing pulses (6 ms, 10 kHz). Diffusion gradient pulses were positioned symmetrically around both 180°pulses; δ = 10 ms, Δ = 30 ms. Only gradient amplitudes were varied to change the diffusion weighting or *b*-value and were applied in the transverse direction, i.e., G_x or G_y. A crusher pulse (4 G cm^{-1}, 0.4 ms) was played after acquisition to dephase any remaining transverse magnetization. As is typical for hyperpolarized experiments, no signal averaging was used.

2.5. Extra- and intracellular weighted diffusion coefficients of hyperpolarized ^{13}C metabolites

To measure the diffusion coefficient of predominantly extra- and intracellular weighted hyperpolarized ^{13}C metabolites, a gradient array was used where the highest *b*-values were acquired before smaller *b*-values (Fig. 1b), thereby exploiting the strong hyperpolarized signal at the beginning of the experiment. Signal modulation due to T_1 decay, repeated excitations from a single, non-renewable pool of magnetization and metabolism was removed with normalization scans that were interspersed throughout the gradient array. These normalization scans ensured that the normalized signal losses were predominantly due to diffusion weighting. This approach is similar to that of a previous study [12], where every diffusion weighted acquisition at the spin-echo (S_{echo}) was also normalized by a non-diffusion weighted signal acquired immediately after excitation (S_{FID}). The equation to determine the diffusion coefficients becomes

$$\ln(S_i') = -b \cdot D \tag{3}$$

where S' is the normalized diffusion weighted signal, defined by

$$S_i' = \frac{S_i \cdot \cos^{-1}(\theta)}{S_{0+}} \text{ or } S_i' = \frac{S_i}{S_{0-} \cdot \cos^{-1}(\theta)} \tag{4}$$

depending on whether the closest normalizing scan is either immediately before (S_{0+}) or after (S_{0-}) the normalized signal (S_i'). Normalizing scans S_{0+} and S_{0-} had G = 1 G cm^{-1} and *b*-value = 2.4 s mm^{-2}. The cosine factor corrects for the difference in magnetization between S_i and S_{0+} or S_{0-} due to multiple excitations from a single, non-renewable pool of magnetization. These normalizations reduce non-diffusion weighted signal changes. For these experiments, θ = 30°, G = 1–80 G cm^{-1}, *b*-value = 2–15,000 s mm^{-2}, TR = 0.5 s, TE = 79.8 ms.

As for the proton diffusion coefficient measurements, the extra- and intracellular weighted diffusion coefficients of the hyperpolarized ^{13}C metabolites were determined by fitting the fast and slowly decaying asymptotes. Specifically, after normalizing the signal at each *b*-value (i.e., S_i'), the first 7 or the last 5 points were fit with Eq. (3). This set of experiments was performed in quadruplicates.

The same statistical tests were used to compare the extra- and intracellular diffusion coefficients of these hyperpolarized ^{13}C metabolites as those used to compare the water diffusion coefficients, explained above.

2.6. Assessment of real-time membrane transport of hyperpolarized ^{13}C lactate

Using diffusion weighting, the extra- and the intracellular weighted hyperpolarized ^{13}C metabolite pools were monitored over time for UOK262 cells. This was accomplished through a two-step process. First, the metabolite signals were acquired with alternating low and high diffusion weighting. This was followed by,

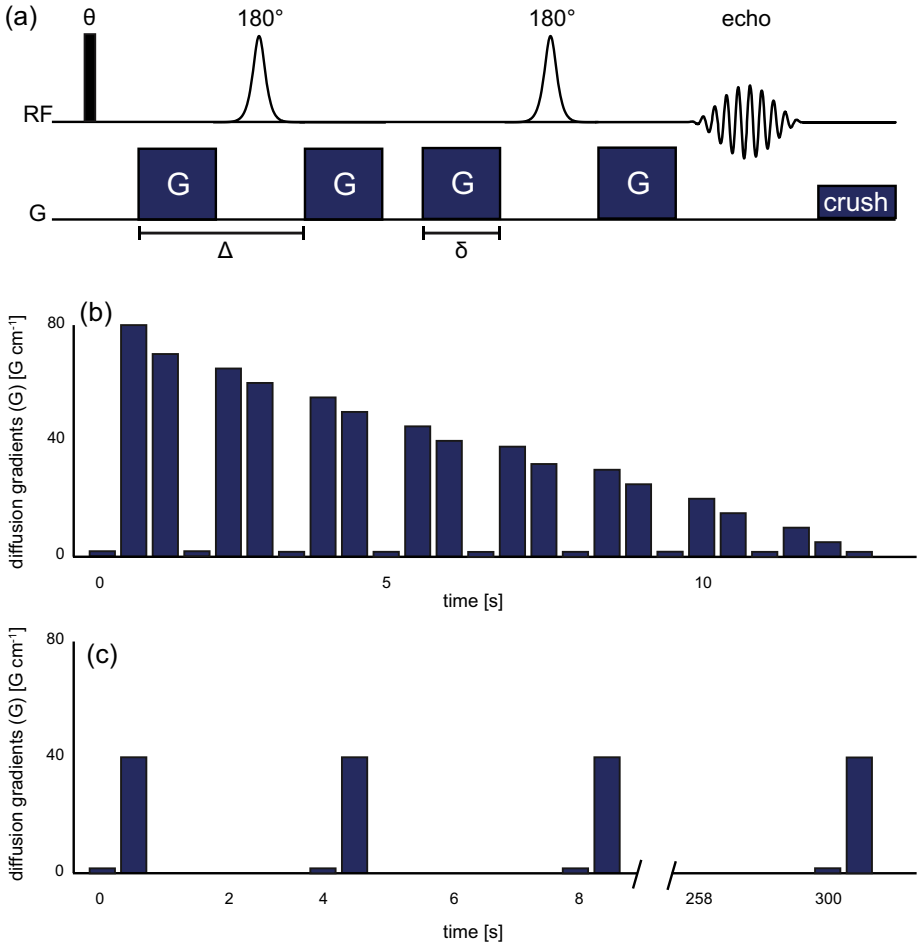

Fig. 1. (a) The pulsed gradient double spin echo sequence used for diffusion weighting of hyperpolarized ^{13}C metabolites. Diffusion gradients (G) are placed symmetrically around the adiabatic 180° refocusing pulses, with a duration δ and a separation Δ. A crusher gradient after the readout ensures no transverse magnetization carries-over to subsequent scans. The excitation flip angle θ was either 15° or 30°. (b) The diffusion gradient array used to measure the extra- and intracellular weighted diffusion coefficients of hyperpolarized ^{13}C metabolites. Every third scan (*small boxes*) was used to normalize adjacent diffusion weighted scans (*large boxes*), thereby removing the effects of T_1 relaxation and metabolism on the signal change from that due to the diffusion weighting. (c) The gradient array used to measure the change in the total (*small boxes*) and the intracellular weighted (*large boxes*) hyperpolarized ^{13}C metabolite pools over time. See methods for a more detailed description of these two acquisition schemas.

solving for the extra- and intracellular signals using both the signals at low and high diffusion weighting and the previously measured diffusion coefficients for these metabolites.

The pulse sequence consisted of low and high b-value scans in succession, after which a 3 s delay was inserted before the next pair of acquisitions (Fig. 1c). The pulsed gradient double spin echo sequence was used for these acquisitions: $\theta = 15°$, TR = 0.5 s, TE = 79.8 ms, low b-value = 2.4 s mm^{-2} at $G = 1$ G cm^{-1}, high b-value = 3863 s mm^{-2} at $G = 40$ G cm^{-1}, $\delta = 10$ ms, $\Delta = 30$ ms, delay between paired low and high b-value scans = 3 s, total acquisition time = 300 s.

The diffusion gradients of the low b-value scans, 2.4 s mm^{-2}, merely act as crusher gradients around each of the adiabatic refocusing pulses and didn't impart significant diffusion weighting. The diffusion weighting necessary to observe predominantly the intracellular signal was chosen by identifying a b-value where, under flowing conditions in the bioreactor, the hyperpolarized ^{13}C pyruvate hydrate signal that had been injected into cell-free alginate microspheres was below the noise level, namely a b-value = 3863 s mm^{-2}. The suppression of hyperpolarized ^{13}C pyruvate hydrate was chosen because its signal intensity is in the same order of magnitude as the ^{13}C lactate signal.

Given the dynamic metabolite signals at low (S_{low}) and high (S_{high}) b-values, the extra- (S_{extra}) and intracellular (S_{intra}) signals were determined by solving the two simultaneous equations:

$$S_{low} = S_{intra}\exp(-b_{low}\cdot D_{in}) + S_{extra}\exp(-b_{low}\cdot D_{extra}) \quad (5)$$

$$S_{high} = S_{intra}\exp(-b_{high}\cdot D_{in}) + S_{extra}\exp(-b_{high}\cdot D_{extra}) \quad (6)$$

where D_{extra} and D_{in} are the extra- and intracellular weighted diffusion coefficients for either pyruvate or lactate for the UOK262 cells, as reported in Table 1. These equations assume a two-compartment model, where metabolites reside in only one of two diffusion environments.

The conversion of hyperpolarized ^{13}C pyruvate to lactate was assessed by taking the ratio

$$\frac{L_{total}}{P_{total}} \approx \frac{\sum_{n=1}^{N} L(n)}{\sum_{n=1}^{N} P(n)} \quad (7)$$

where L_{total} and P_{total} are the sum of the signals at all time points (i.e., the area under the curve) acquired here for the total signal at the low b-value (S_{low}). This ratio has previously been shown to correlate with k_{PL} measurements made with models of the rate of enzymatic conversion of lactate dehydrogenase (LDH) [29].

Using a similar approach, the distribution of the hyperpolarized ^{13}C metabolite pools during the time course of the experiment was assessed by taking the ratios of the various metabolite pools

$$\frac{X_{intra}}{X_{total}} \text{ and } \frac{X_{intra}}{X_{extra}} \quad (8)$$

Table 1
Diffusion coefficients (D) of ^{1}H water and hyperpolarized ^{13}C metabolites at 37 °C, as measured in the bioreactor (±SD, $N = 4$).

	^{1}H water	Hyperpolarized ^{13}C pyruvate	Hyperpolarized ^{13}C lactate
Extracellular ADC [$\times 10^{-3}$ mm^2 s^{-2}]			
Microspheres	3.27 ± 0.13	1.26 ± 0.10	1.04 ± 0.08
UMRC6	2.86 ± 0.11*	1.20 ± 0.11	0.63 ± 0.06*
UOK262	2.97 ± 0.03*	1.19 ± 0.06	0.57 ± 0.10*
Intracellular ADC [$\times 10^{-3}$ mm^2 s^{-2}]			
UMRC6	0.15 ± 0.006	0.17 ± 0.02	0.17 ± 0.03
UOK262	0.12 ± 0.002**	0.10 ± 0.007**	0.19 ± 0.03

* Statistically different from diffusion coefficients measured in the microspheres, p-value < 0.05.
** Statistically different from diffusion coefficients measured in the UMRC6 cells, p-value < 0.05.

where X represents the sum of the signal for pyruvate (P) or lactate (L). These ratios were normalized to the number of cells used for each experiment, as measured by ^{31}P spectroscopy and previously described in [7].

After several hyperpolarized ^{13}C acquisitions, the same batch of cells were treated with 1 mM 4,4′-Di-isothiocyanostilbene-2,2′-disulphonic acid (DIDS), an inhibitor of monocarboxylate transporters (MCTs) [8], within the bioreactor for 40 min before injection of the hyperpolarized solution to modulate the extra- and intracellular distribution of lactate pools. To clearly see the relative change in the ratios before and after treatment, the pre-treatment data was normalized to 1.

For these experiments, a paired two-tailed t-test was used for all statistical comparisons with a significance level (α) of 0.05. All values are represented as mean ± standard deviation. These experiments were performed in triplicates. Normality was tested with the Shapiro–Wilk test. All statistical comparisons were done in R, version 3.2.4.

3. Results

3.1. Extra- and intra-cellular weighted diffusion coefficients of ^{1}H water

Measuring water signal of the cells encapsulated in the alginate microspheres over a range of b-values reveals a multi-exponential signal decay (Fig. 2a). The self-diffusion of water is represented by the fast asymptote (dashed line), while the water within the cells is represented by the slow asymptote (dotted line), as has been previously described for bioreactor cell experiments [16]. The open markers in Fig. 2a are the water signal from cell-free alginate microspheres and show no signal at higher b-values, given the absence of an intracellular environment. At mid-range b-values (i.e., 4000–6000 s mm^{-2}) the presence of the water within the alginate microspheres can be seen by the slight trailing-off of the curve, as has been previously described [28]. However, there are not enough data points with sufficient signal-to-noise at higher b-values to calculate the diffusion coefficient of water in the cell-free alginate microspheres. The extra- and intracellular weighted diffusion coefficients of water are listed in Table 1. The extracellular weighted diffusion coefficients for water measured in the cell-free microspheres is significantly greater than that measured in either of the experiments with microspheres with cells (the p-value < 0.005), which may be indicative of slight differences in the packing of the microspheres or the structure of the alginate itself when cells are present. Also, the intracellular weighted diffusion coefficients of water for UMRC6 and UOK262 cells are significantly different (p-value = 5.7 × 10^{-5}), which may be due to differences in the intracellular structure of these two cell lines.

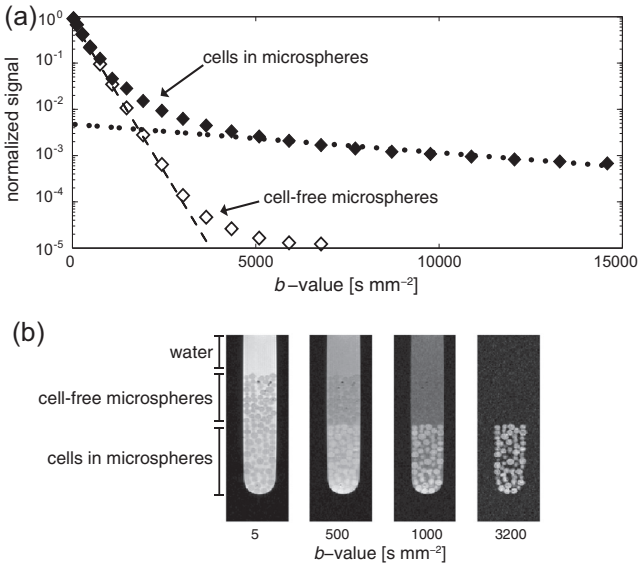

Fig. 2. (a) The water signal response with increasing diffusion weighting in the bioreactor. For cells encapsulated in the alginate microspheres (◆), the water signal response reveals the presence of multiple environments with different water diffusion coefficients. The fast and slow asymptotes (*dotted lines*) were used to determine extra- and intracellular weighted diffusion coefficients, respectively. The water signal response in cell-free microspheres (◇) reflects water diffusion in solution and in the microspheres. (b) A diffusion weighted imaging experiment confirms the presence of the different diffusion environments. At low b-values, water signal is present in all three environments. As the b-values increase, signal from compartments with faster diffusion decreases while signal from highly restricted environments (i.e., intracellular) persists. At b-values above 3200 s mm^{-2}, only signal from within the cells can be seen. The intensity of these images are scaled independently to more easily identify the various features. Only in this imaging experiment were alginate microspheres with and without cells layered for a single experiment; all other experiments acquired either with one or the other.

The diffusion weighted imaging experiment, shown in Fig. 2b, visually confirms the suppression of extracellular water signal with increasing b-values. Shown is an NMR tube with three regions: only water, cell-free microspheres and cells encapsulated within the alginate microspheres. In the images, only intracellular water signal remains at merely 3200 s mm^{-2}, which is lower than that indicated by the graph in Fig. 2a acquired spectroscopically. This discrepancy most likely arises because of the lower sensitivity of the imaging sequence.

3.2. Extra- and intracellular weighted diffusion coefficients of hyperpolarized ^{13}C metabolites

As for the water signal, the diffusion coefficients of the hyperpolarized ^{13}C metabolites can be determined in the extra- and intracellular environments within the bioreactor. Yet, in the case of hyperpolarized ^{13}C metabolite signal, several sources of signal change are present that will complicate the quantification of diffusion coefficients. These include the decay of the hyperpolarized signal due to T_1, repeatedly using the signal from a single, non-renewable pool of magnetization and metabolism. To reduce the effects of these non-diffusion weighted signal changes, multiple normalization scans were acquired throughout the experiment. The result gives a multi-exponential signal response where, like for the water measurements, the fast and slow asymptotes correspond to the extra- and intracellular diffusion coefficients, as seen in Fig. 3a. All extra- and intracellular weighted diffusion coefficients of the hyperpolarized ^{13}C metabolites are listed in Table 1.

To confirm the ability to measure purely intracellular hyperpolarized ^{13}C metabolite signal, the signal decay of these same

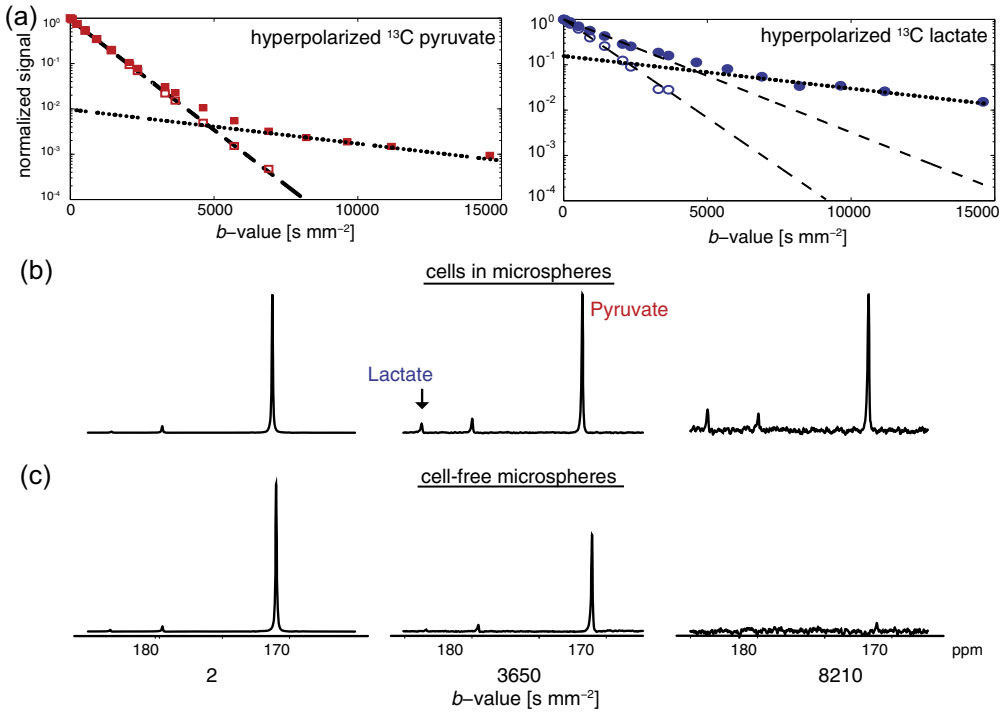

Fig. 3. (a) Hyperpolarized ^{13}C metabolite signal response with increasing diffusion weighting in the bioreactor. The multi-exponential signal response of hyperpolarized ^{13}C pyruvate and lactate reveals multiple diffusion environments in experiments with UOK262 cells encapsulated in alginate microspheres (*filled symbols*). The fast and slow asymptotes were used to determine the diffusion coefficients in the extra- and intracellular weighted environments, respectively similar to that of proton in Fig. 2. Diffusion weighting of the injected hyperpolarized ^{13}C substrates in cell-free microspheres are also shown (*empty symbols*). Hyperpolarized ^{13}C lactate in cell experiments was produced by conversion from pyruvate while in the cell-free microsphere experiment ^{13}C lactate was polarized and injected. Spectra of the hyperpolarized ^{13}C pyruvate and lactate with increasing diffusion weighting (*b*-value) shows the suppression of extracellular signals at higher *b*-values in cells encapsulated in alginate (b) and in cell-free microspheres (c). For (b) and (c) spectra at a single *b*-value are scaled to the same SNR.

compounds was measured in cell-free alginate microspheres. The spectra shown in Fig. 3b and c clearly show the absence of the hyperpolarized metabolites at a high *b*-value of 8210 s mm^{-2} in the cell-free alginate microspheres, confirming, that the observed signals in the cells arises predominantly from the intracellular compartment. At lower *b*-values, Table 1 and Fig. 3a show that the extracellular diffusion coefficient, i.e., fast signal decay rate, for hyperpolarized ^{13}C pyruvate is similar between experiments with and without cells in the microspheres (p-value = 0.58 for the ANOVA). While the extracellular diffusion coefficient of hyperpolarized ^{13}C lactate is different between cell-free microspheres and the experiments with encapsulated cells (p-value < 0.005), the extracellular diffusion coefficients in both the UOK262 and UMRC6 cells experiments are similar. These smaller extracellular lactate diffusion coefficients in the experiments with cells may be due to localization of the dominant hyperpolarized ^{13}C lactate signal. In the cell-free microsphere experiment, ^{13}C lactate was polarized and injected into the bioreactor, thereby being predominantly in the media and resulting in a higher extracellular diffusion coefficient (Table 1). Also, the diffusion coefficients of lactate and pyruvate measured in cell free microspheres are comparable suggesting that these two injected hyperpolarized substrates with similar molecular weights are in similar environments. However, in the cell encapsulates, the hyperpolarized ^{13}C lactate was produced within the cells and transported into the extracellular environment during the experiment, thus most likely being localized within the extracellular matrix immediately laid-down by the cells. This may result in a lower extracellular weighted diffusion coefficient (Table 1) than ^{13}C lactate in free solution. Table 1 shows that while the intracellular weighted diffusion coefficients for pyruvate are slightly different between the two cell lines (p-value < 0.005), those for lactate are similar (p-value = 0.48).

3.3. Assessing extra- and intracellular pools of hyperpolarized ^{13}C lactate

To measure the dynamic extra- and intracellular hyperpolarized ^{13}C metabolite pools over the time course of the experiments, the metabolite signals were intermittently measured with low and high degrees of diffusion weighting and subsequently solved for the extra- and intracellular components using a two-compartment approach. UOK262 cells were used for this experiment because they are known to transport relatively large amounts of lactate out into the extracellular environment [7,8]. Fig. 1c shows the diffusion gradient array used for these measurements.

The dynamic distribution of hyperpolarized ^{13}C pyruvate and lactate between the extra- and intracellular compartments for the UOK262 cells can be seen in Fig. 4. Considering that hyperpolarized ^{13}C pyruvate is injected at excess into the bioreactor, its intracellular fraction is small compared to the extracellular fraction. Fig. 4b shows the intracellular fraction is about 1% of the extracellular signal, which can also be seen in Fig. 3a as the ratios of the intercepts for the fast and slow asymptotes. Contrary to hyperpolarized ^{13}C pyruvate, extracellular hyperpolarized ^{13}C lactate was first produced in the cells and then actively transported out via MCT4. This results in a substantially different extra- to intracellular distribution of hyperpolarized ^{13}C lactate in the UOK262 cells, as seen in Fig. 4c that shows the intracellular fraction to be about 20% of the extracellular fraction. This ratio can also be seen in Fig. 3b as the ratio of the intercepts for the fast and slow asymptotes.

Treatment of the UOK262 cells with 1 mM of the MCT inhibitor DIDS shows clear increase in the intracellular hyperpolarized ^{13}C lactate pool relative to the extracellular pool, as illustrated by the reduced differential area (grayed area in Fig. 4c and d). DIDS has

been shown to inhibit MCT4 more readily than MCT1 [30], the dominant transporters for lactate efflux and pyruvate uptake [31], respectively.

The overall extra- and intracellular distribution of these hyperpolarized ^{13}C metabolites was assessed by taking the ratios X_{intra}/X_{total}, X_{intra}/X_{extra}, and X_{intra}/X_{intra}, where X represents the metabolites pyruvate (P) or lactate (L). The distribution of hyperpolarized ^{13}C pyruvate did not significantly change with treatment of DIDS (p-value = 0.21 for both P_{intra}/P_{total} and P_{intra}/P_{extra}, respectively). However, the 2.3-fold increase of the relative intracellular fraction of hyperpolarized ^{13}C lactate with DIDS treatment is significant (p-value = 0.01 for both L_{intra}/L_{total} and L_{intra}/L_{extra}, respectively). This is predominantly due to the reduced lactate efflux by DIDS, which has a high affinity for blocking MCT4. Fig. 5 also shows that the conversion of hyperpolarized ^{13}C pyruvate to lactate decreases with DIDS treatment, as demonstrated by the decrease in the ratios L_{total}/P_{total} and L_{extra}/P_{extra} (p-value = 0.01 for both). This may result from increased intracellular lactate concentration that inhibits the conversion of pyruvate to lactate via LDH [32].

All of the ratios including P_{intra} have a large variance and do not show a significant change with DIDS treatment. This large variance is most likely due to the difficultly in measuring signal changes of the relatively tiny intracellular fraction of the injected hyperpolarized ^{13}C pyruvate (about 1% of the extracellular fraction).

4. Discussion

4.1. Extra- and intracellular weighted diffusion coefficients

As previous studies of cells in bioreactors have shown, acquiring signal from metabolites with increasing diffusion weighting results in a multi-exponential signal response, where the fast and slowly decaying asymptotes represent the extra- and intracellular diffusion coefficients of the molecule under study [16]. The water diffusion coefficients measured in the extracellular environments ($3.27 \pm 0.13 \times 10^{-3}$ mm^{-2} s at 37 °C) align nicely with those values previously published of 2.919 and 2.895×10^{-3} mm^{-2} s (at 35 °C) [33,34]. Likewise, the intracellular weighted water diffusion coefficients measured ($0.12–0.15 \pm 0.006 \times 10^{-3}$ mm^{-2} s) also align with those measured previously of 0.11×10^{-3} mm^{-2} s [16,35]. The main purpose of these water diffusion coefficient measurements was to validate a previously established methodology on our system in order to measure the extra- and intracellular diffusion coefficients of hyperpolarized ^{13}C metabolites.

It is challenging to measure diffusion coefficients of hyperpolarized ^{13}C molecules due to the multiple sources of signal change, including T_1 decay, repeated excitations from a single, non-renewable pool of magnetization and metabolism. Previous studies have quantified these non-diffusion related signal changes and corrected the diffusion weighted acquisitions accordingly [10,11]. To simplify the quantification of the diffusion coefficients, multiple interspersed normalization scans were acquired temporally close to the diffusion weighted scans and thereby eliminate the effects of these non-diffusion weighted signal changes. This methodology was verified in solution studies of hyperpolarized ^{13}C urea, where diffusion coefficients measured via this technique aligned with those measured previously that corrected for T_1 signal loss [10]. This dynamic normalization approach is also similar to a previous study where every diffusion weighted acquisition (S_{echo}) was normalized by the non-diffusion weighted signal acquired immediately after excitation (S_{FID}) [12]. In the encapsulated cell experiments, this produces multi-exponential curves for these

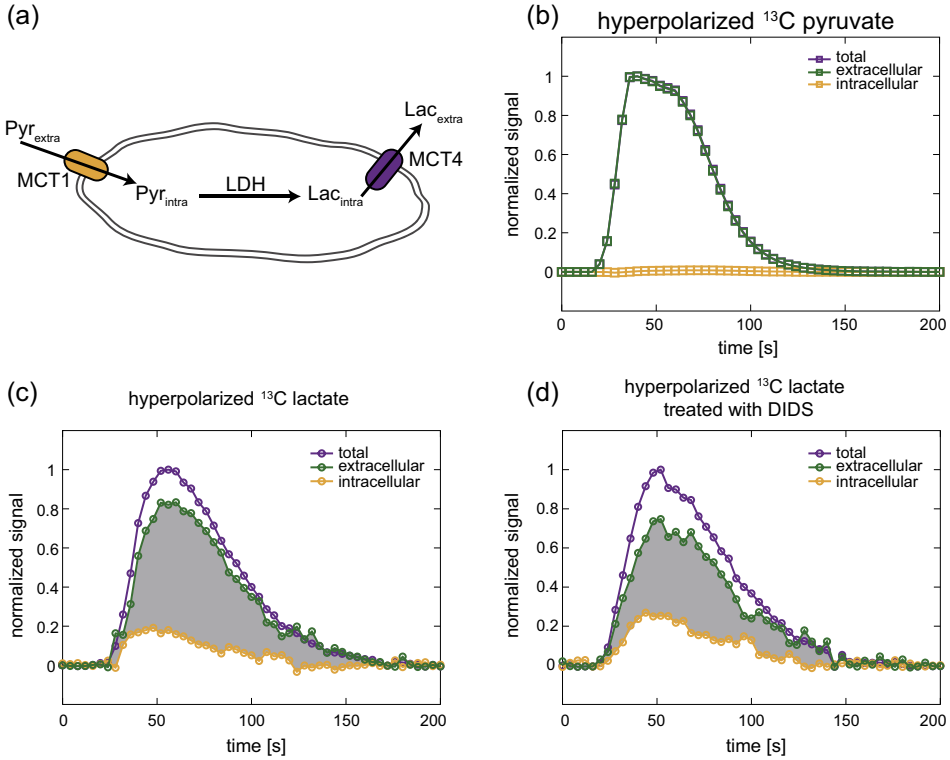

Fig. 4. (a) A schematic of a cell showing the transport of hyperpolarized ^{13}C pyruvate into the cell via the monocarboxylate transporter 1 (MCT1), its conversion to hyperpolarized ^{13}C lactate by the enzyme lactate dehydrogenase (LDH) and the transport of ^{13}C lactate out of the cell via MCT4. The dynamic signals of hyperpolarized ^{13}C pyruvate (b) and lactate (c) in UOK262 cells perfused in the bioreactor, showing the total, extra- and intracellular metabolite pools. The total and intracellular signals are acquired at intermittent low and high b-values, namely 2.4 and 3863 s mm^{-2} respectively. (d) UOK262 cells treated with the high-affinity MCT4 inhibitor DIDS show an increase in the fraction of intracellular hyperpolarized ^{13}C lactate relative to the extracellular hyperpolarized ^{13}C lactate. The change in shaded area in (c) and (d) between the extra- and intracellular hyperpolarized ^{13}C lactate curves highlights the relative changes in these lactate pools due to the treatment with DIDS. All plots are normalized to the maximum total signal of the respective hyperpolarized metabolite.

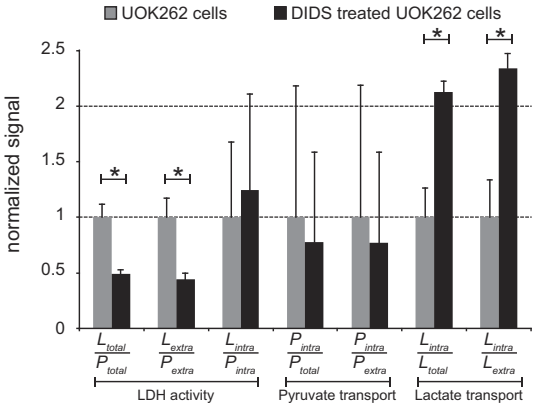

Fig. 5. The relative changes in metabolism and membrane transport of hyperpolarized ^{13}C metabolites in UOK262 cells, without and with treatment with DIDS, a high-affinity inhibitor of MCT4. The ratios that reflect LDH activity, or conversion of hyperpolarized ^{13}C pyruvate to ^{13}C lactate, show a significant decrease with DIDS treatment. The membrane transport ratios for hyperpolarized ^{13}C pyruvate do not significantly change with DIDS treatment. The increase in the lactate transport ratios shows that DIDS inhibition of MCT4 leads to a higher intracellular fraction of hyperpolarized ^{13}C lactate. Significant differences with p-value < 0.05 are represented by *.

hyperpolarized ^{13}C metabolites similar to those for water, where the fast and the slowly decaying asymptotes correspond to the extra- and intracellular diffusion coefficients.

The extracellular diffusion coefficients for the hyperpolarized ^{13}C metabolites, as measured in the cell-free microspheres, correspond well with those measured previously in solution [10] when accounting for difference in temperature and the more restricted environment of the alginate. Previous cell suspension studies [11] of the diffusion coefficients of hyperpolarized ^{13}C pyruvate, pyruvate hydrate and lactate with b-values up to ~1500 s mm^{-2} measured diffusion coefficients of these molecules approximately equal to those measured here in the extracellular space (Table 1). The low b-values used in that study were not sufficient to measure purely intracellular diffusion coefficients. All other currently published studies reporting hyperpolarized ^{13}C metabolite diffusion coefficients were acquired *in vivo* [12–14,36] and also used lower b-values than those used in this study. The reported coefficients were between the extra- and intracellular values measured in this study (Table 1). The diffusion coefficients measured *in vivo* thus represent the combined effects of both the extracellular tissue and the intracellular environments. Similarly, water measurements in tissue are higher than those listed in Table 1 for intracellular water [37]. The intracellular weighted diffusion coefficients for the hyperpolarized ^{13}C lactate is similar to that measured previously *in vivo* in rat brain using an infusion of thermally polarized ^{13}C lactate, a {^{1}H–^{13}C} editing technique and b-values up to 50,000 s mm^{-2} [38]. The extra- and intracellular weighted metabolite diffusion coefficients measured in this *in vitro* bioreactor study can be used to better interpret ADC measurements of hyperpolarized ^{13}C lactate *in vivo*, which are a function of both the proportion of extra- and intracellular lactate as well as changes in the tissue microenvironment.

4.2. Assessment of membrane transport of hyperpolarized ^{13}C metabolites

The same study that motivated the extra- and intracellular diffusion coefficient measurements [16] also showed the ability to measure membrane transport by observing the total and intracellular signals, each at a pre-specified b-value, over time. With hyperpolarized ^{13}C metabolites, the signal is sufficiently large for measurements to be made in real-time and without the need to average signals for prolonged periods of time, as is necessary for the thermal NMR measurements. When the metabolite signals at high and low b-value are observed in time, the change in the extra- and intracellular metabolite pools can be measured in real-time.

The dynamic changes in extra- and intracellular hyperpolarized ^{13}C lactate observed in this study was consistent with substantial efflux of lactate out of UOK262 cells within the time-frame of the hyperpolarized MR study. This finding is consistent with a prior published MR compatible cell culture bioreactor study of UOK262 cells, in which flow-rate modulations in the bioreactor demonstrated that hyperpolarized ^{13}C lactate was transported out of the cell and washed-away during the time frame of the hyperpolarized MR study [7]. Furthermore, a recent publication studying UOK262 cells in a 5 mm MR compatible bioreactor, which enabled a spectral line-width narrow enough for the separation of the intra- and extracellular hyperpolarized ^{13}C lactate peaks, showed that when subjected to DIDS inhibition, the ratio of intra- to extracellular lactate increased by 1.64-fold [8]. This study showed a 2.35-fold increase in the intra- to extracellular lactate ratio with DIDS inhibition (Fig. 5). The difference between these two observations may arise from limitations in each of the measurements. Both studies assumed a two-compartment model with an extra- and intracellular space, but in reality there are likely a greater variety of compartments, particularly in the extracellular space where metabolites are found in free-solution and in the alginate microspheres, both near and far from the cell. Inconsistent assignment of additional compartments into either the intra or extracellular space between the studies would in turn lead to the differences measured. This study assumes that only two compartments with distinct diffusion environments exist, namely those characterized by the extra- and intracellular diffusion coefficients (Table 1). Additional compartments will be assigned to either the extra- or intracellular space depending on their diffusion characteristics.

MCTs are a class of transporters that shuttle various monocarboxylates across the cell membrane, coupled with the transport of a proton. MCT1 exhibits higher affinity for pyruvate influx, while MCT4 facilitates lactate efflux [31]. It is well established that many malignant cancers exhibit an upregulation of MCT4 [39], such as in breast cancer [5] and are even correlated with tumor grade as has been shown in RCCs [6,40] and prostate cancer [41]. In cancer cells, the role of MCT4 in shunting lactate and protons form the intracellular environment helps maintain an intracellular physiologic pH while acidifying the extracellular space and thereby promotes invasion into the surrounding tissue [42,43]. The studies presented here show that ^{13}C lactate generated from hyperpolarized ^{13}C pyruvate is superbly suited to evaluate the efflux of lactate from cancer cells. More studies are needed to evaluate the differences in hyperpolarized ^{13}C lactate efflux in normal, indolent and metastatic cancer cells. In a clinical setting, this would allow for a more refined characterization of cancer cells, where evaluations would incorporate both the extent of hyperpolarized ^{13}C lactate production and its distribution.

5. Conclusion

We developed a method to reliably measure intracellular diffusion coefficients of hyperpolarized ^{13}C metabolites via large diffusion weighting. This was achieved with a pulsed gradient double spin echo sequence with strong diffusion gradient amplitudes allowed for b-values up to 15,000 s mm^{-2} to be achieved. Furthermore, by employing alternating low and high b-values allowed the real-time assessment of the extra- and intracellular hyperpolarized ^{13}C metabolite pools. The ^{13}C metabolite diffusion coefficients measured in this study may facilitate the design and interpretation

of *in vivo* diffusion weighted hyperpolarized ^{13}C experiments in order to probe membrane transport. Given the correlation of MCT4 with pathologic cancer grade and in promoting tumor invasion, diffusion weighted hyperpolarized ^{13}C MR may provide important additional information that results in improved cancer risk assessment for individual patients and thereby improves therapeutic selection.

References

[1] S.J. Nelson, J. Kurhanewicz, D.B. Vigneron, P.E.Z. Larson, A.L. Harzstark, M. Ferrone, et al., Metabolic imaging of patients with prostate cancer using hyperpolarized [1-^{13}C]pyruvate, Sci. Transl. Med. 5 (2013) 198ra108, http://dx.doi.org/10.1126/scitranslmed.3006070.

[2] O. Warburg, On the origin of cancer cells, Science 123 (1956) 309–314 (1956 ed.).

[3] M.J. Albers, R. Bok, A.P. Chen, C.H. Cunningham, M.L. Zierhut, V.Y. Zhang, et al., Hyperpolarized ^{13}C lactate, pyruvate, and alanine: noninvasive biomarkers for prostate cancer detection and grading, Cancer Res. 68 (2008) 8607–8615, http://dx.doi.org/10.1158/0008-5472.CAN-08-0749.

[4] G. Kroemer, J. Pouysségur, Tumor cell metabolism: cancer's Achilles' heel, Cancer Cell 13 (2008) 472–482, http://dx.doi.org/10.1016/j.ccr.2008.05.005.

[5] S.M. Gallagher, J.J. Castorino, D. Wang, N.J. Philp, Monocarboxylate transporter 4 regulates maturation and trafficking of CD147 to the plasma membrane in the metastatic breast cancer cell line MDA-MB-231, Cancer Res. 67 (2007) 4182–4189, http://dx.doi.org/10.1158/0008-5472.CAN-06-3184.

[6] M. Gerlinger, C.R. Santos, B. Spencer-Dene, P. Martinez, D. Endesfelder, R.A. Burrell, et al., Genome-wide RNA interference analysis of renal carcinoma survival regulators identifies MCT4 as a Warburg effect metabolic target, J Pathol. 227 (2012) 146–156, http://dx.doi.org/10.1002/path.4006. Blackwell Publishing.

[7] K.R. Keshari, R. Sriram, B.L. Koelsch, M. Van Criekinge, D.M. Wilson, J. Kurhanewicz, et al., Hyperpolarized ^{13}C-pyruvate magnetic resonance reveals rapid lactate export in metastatic renal cell carcinomas, Cancer Res. 73 (2013) 529–538, http://dx.doi.org/10.1158/0008-5472.CAN-12-3461.

[8] R. Sriram, M. Van Criekinge, A. Hansen, Z.J. Wang, D.B. Vigneron, D.M. Wilson, et al., Real-time measurement of hyperpolarized lactate production and efflux as a biomarker of tumor aggressiveness in an MR compatible 3D cell culture bioreactor, NMR Biomed. 28 (2015) 1141–1149, http://dx.doi.org/10.1002/nbm.3354.

[9] D. Le Bihan, E. Breton, D. Lallemand, P. Grenier, E. Cabanis, M. Laval-Jeantet, MR imaging of intravoxel incoherent motions: application to diffusion and perfusion in neurologic disorders, Radiology 161 (1986) 401–407, http://dx.doi.org/10.1148/radiology.161.2.3763909.

[10] B.L. Koelsch, K.R. Keshari, T.H. Peeters, P.E.Z. Larson, D.M. Wilson, J. Kurhanewicz, Diffusion MR of hyperpolarized ^{13}C molecules in solution, Analyst 138 (2013) 1011–1014, http://dx.doi.org/10.1039/c2an36715g.

[11] F. Schilling, S. Düwel, U. Köllisch, M. Durst, R.F. Schulte, S.J. Glaser, et al., Diffusion of hyperpolarized (13) C-metabolites in tumor cell spheroids using real-time NMR spectroscopy, NMR Biomed. 26 (2013) 557–568, http://dx.doi.org/10.1002/nbm.2892.

[12] M.I. Kettunen, B.W.C. Kennedy, D.-E. Hu, K.M. Brindle, Spin echo measurements of the extravasation and tumor cell uptake of hyperpolarized [1-(13) C]lactate and [1-(13) C]pyruvate, Magn. Reson. Med. (2012), http://dx.doi.org/10.1002/mrm.24591.

[13] L.V. Søgaard, F. Schilling, M.A. Janich, M.I. Menzel, J.H. Ardenkjaer-Larsen, In vivo measurement of apparent diffusion coefficients of hyperpolarized ^{13}C-labeled metabolites, NMR Biomed. 27 (2014) 561–569, http://dx.doi.org/10.1002/nbm.3093.

[14] B.L. Koelsch, G.D. Reed, K.R. Keshari, M.M. Chaumeil, R. Bok, S.M. Ronen, et al., Rapid in vivo apparent diffusion coefficient mapping of hyperpolarized (13) C metabolites, Magn. Reson. Med. 74 (2015) 622–633, http://dx.doi.org/10.1002/mrm.25422.

[15] J.E. Tanner, E.O. Stejskal, Restricted self-diffusion of protons in colloidal systems by the pulsed-gradient, spin-echo method, J. Chem. Phys. 49 (1968) 1768–1777.

[16] P.C. Van Zijl, C.T. Moonen, P. Faustino, J. Pekar, O. Kaplan, J.S. Cohen, Complete separation of intracellular and extracellular information in NMR spectra of perfused cells by diffusion-weighted spectroscopy, Proc. Natl. Acad. Sci. U.S.A. 88 (1991) 3228–3232.

[17] B.A. Inglis, E.L. Bossart, D.L. Buckley, E.D. Wirth, T.H. Mareci, Visualization of neural tissue water compartments using biexponential diffusion tensor MRI, Magn. Reson. Med. 45 (2001) 580–587.

[18] H.B. Grossman, G. Wedemeyer, L.Q. Ren, Human renal carcinoma: characterization of five new cell lines, J. Surg. Oncol. 28 (1985) 237–244.

[19] Y. Yang, V.A. Valera, H.M. Padilla-Nash, C. Sourbier, C.D. Vocke, M.A. Vira, et al., UOK 262 cell line, fumarate hydratase deficient (FH−/FH−) hereditary leiomyomatosis renal cell carcinoma: in vitro and in vivo model of an aberrant energy metabolic pathway in human cancer, Cancer Genet. Cytogenet. 196 (2010) 45–55, http://dx.doi.org/10.1016/j.cancergencyto.2009.08.018.

[20] K. Keshari, J. Kurhanewicz, R. Jeffries, D. Wilson, B. Dewar, M. Van Criekinge, et al., Hyperpolarized ^{13}C spectroscopy and an NMR-compatible bioreactor system for the investigation of real-time cellular metabolism, Magn. Reson. Med. 63 (2010) 322–329.

[21] P. Chandrasekaran, C. Seagle, L. Rice, J. Macdonald, D.A. Gerber, Functional analysis of encapsulated hepatic progenitor cells, Tissue Eng. 12 (2006) 2001–2008, http://dx.doi.org/10.1089/ten.2006.12.2001.

[22] E.O. Stejskal, J.E. Tanner, Spin diffusion measurements: spin echoes in the presence of a time-dependent field gradient, J. Chem. Phys. 42 (1965) 288–292, http://dx.doi.org/10.1063/1.1695690. AIP Publishing.

[23] J.H. Ardenkjaer-Larsen, B. Fridlund, A. Gram, G. Hansson, L. Hansson, M.H. Lerche, et al., Increase in signal-to-noise ratio of >10,000 times in liquid-state NMR, Proc. Natl. Acad. Sci. U.S.A. 100 (2003) 10158–10163, http://dx.doi.org/10.1073/pnas.1733835100.

[24] C. Morze von, R.A. Bok, G.D. Reed, J.H. Ardenkjaer-Larsen, J. Kurhanewicz, D.B. Vigneron, Simultaneous multiagent hyperpolarized (13) C perfusion imaging, Magn. Reson. Med. 72 (2013) 1599–1609, http://dx.doi.org/10.1002/mrm.25071.

[25] D. Mayer, Y.-F. Yen, S. Josan, J.M. Park, A. Pfefferbaum, R.E. Hurd, et al., Application of hyperpolarized [1-^{13}C]lactate for the in vivo investigation of cardiac metabolism, NMR Biomed. 25 (2012) 1119–1124, http://dx.doi.org/10.1002/nbm.2778.

[26] S. Conolly, D. Nishimura, A. Macovski, A selective adiabatic spin-echo pulse, J. Magn. Reson. 83 (1989) 324–334.

[27] C.H. Cunningham, A.P. Chen, M.J. Albers, J. Kurhanewicz, R.E. Hurd, Y.F. Yen, et al., Double spin-echo sequence for rapid spectroscopic imaging of hyperpolarized ^{13}C, J. Magn. Reson. 187 (2007) 357–362, http://dx.doi.org/10.1016/j.jmr.2007.05.014 (2007 ed.).

[28] U. Pilatus, H. Shim, D. Artemov, D. Davis, P.C. Van Zijl, J.D. Glickson, Intracellular volume and apparent diffusion constants of perfused cancer cell cultures, as measured by NMR, Magn. Reson. Med. 37 (1997) 825–832.

[29] D.K. Hill, M.R. Orton, E. Mariotti, J.K.R. Boult, R. Panek, M. Jafar, et al., Model free approach to kinetic analysis of real-time hyperpolarized ^{13}C magnetic resonance spectroscopy data, PLoS ONE 8 (2013) e71996, http://dx.doi.org/10.1371/journal.pone.0071996.

[30] K.S. Dimmer, B. Friedrich, F. Lang, J.W. Deitmer, S. Bröer, The low-affinity monocarboxylate transporter MCT4 is adapted to the export of lactate in highly glycolytic cells, Biochem. J. 350 (Pt 1) (2000) 219–227.

[31] C. Pinheiro, A. Longatto-Filho, J. Azevedo-Silva, M. Casal, F.C. Schmitt, F. Baltazar, Role of monocarboxylate transporters in human cancers: state of the art, J. Bioenergy Biomembr. 44 (2012) 127–139, http://dx.doi.org/10.1007/s10863-012-9428-1. Springer, US.

[32] C. Leon Swisher, B. koelsch, S. Sukumar, R. Sriram, R.D. Santos, Z.J. Wang, et al., Dynamic UltraFast 2D EXchange SpectroscopY (UF-EXSY) of hyperpolarized substrates, J. Magn. Reson. 257 (2015) 102–109, http://dx.doi.org/10.1016/j.jmr.2015.05.011.

[33] R. Mills, Self-diffusion in normal and heavy water in the range 1–45 deg, J. Phys. Chem. 77 (1973) 685–688. ACS Publications. Available: <http://pubs.acs.org/doi/abs/10.1021/j100624a025>.

[34] M. Holz, S.R. Heil, A. Sacco, Temperature-dependent self-diffusion coefficients of water and six selected molecular liquids for calibration in accurate ^{1}H NMR PFG measurements, Phys. Chem. Chem. Phys. 2 (2000) 4740–4742, http://dx.doi.org/10.1039/b005319h.

[35] J. Pfeuffer, W. Dreher, E. Sykova, D. Leibfritz, Water signal attenuation in diffusion-weighted ^{1}H NMR experiments during cerebral ischemia: influence of intracellular restrictions, extracellular tortuosity, and exchange, Mag. Reson. Imag. 16 (1998) 1023–1032, http://dx.doi.org/10.1016/S0730-725X(98)00107-6. Elsevier.

[36] P.S. Patrick, M.I. Kettunen, S.S. Tee, T.B. Rodrigues, E. Serrao, K.N. Timm, et al., Detection of transgene expression using hyperpolarized (13) C urea and diffusion-weighted magnetic resonance spectroscopy, Magn. Reson. Med. (2014), http://dx.doi.org/10.1002/mrm.25254.

[37] C.A. Clark, D. Le Bihan, Water diffusion compartmentation and anisotropy at high b values in the human brain, Magn. Reson. Med. 44 (2000) 852–859.

[38] J. Pfeuffer, J.C. Lin, L. Delabarre, K. Uğurbil, M. Garwood, Detection of intracellular lactate with localized diffusion {^{1}H-^{13}C}-spectroscopy in rat glioma in vivo, J. Magn. Reson. 177 (2005) 129–138, http://dx.doi.org/10.1016/j.jmr.2005.07.010.

[39] M.S. Ullah, A.J. Davies, A.P. Halestrap, The plasma membrane lactate transporter MCT4, but not MCT1, is up-regulated by hypoxia through a HIF-1alpha-dependent mechanism, J. Biol. Chem. 281 (2006) 9030–9037, http://dx.doi.org/10.1074/jbc.M511397200.

[40] R. Sriram, M. Van Criekinge, Santos.J. DeLos, K.R. Keshari, D.M. Peehl, Z.J. Wang, Non-invasive differentiation of benign renal tumors from clear cell renal cell carcinomas using clinically translatable hyperpolarized ^{13}C pyruvate magnetic resonance, Tomography 2 (2016) 35–42, http://dx.doi.org/10.18383/j.tom.2016.00106.

[41] N. Pértega-Gomes, J.R. Vizcaíno, J. Attig, S. Jurmeister, C. Lopes, F. Baltazar, A lactate shuttle system between tumour and stromal cells is associated with poor prognosis in prostate cancer, BMC Cancer 14 (2014) 352, http://dx.doi.org/10.1186/1471-2407-14-352.

[42] B.A. Webb, M. Chimenti, M.P. Jacobson, D.L. Barber, Dysregulated pH: a perfect storm for cancer progression, Nat. Rev. Cancer 11 (2011) 671–677, http://dx.doi.org/10.1038/nrc3110.

[43] C. Stock, A. Schwab, Protons make tumor cells move like clockwork, Pflugers Arch. – Eur. J. Physiol. 458 (2009) 981–992, http://dx.doi.org/10.1007/s00424-009-0677-8.